

## Mikro nepravilnosti kovinskih površin

### Micro-Irregularities of Metal Surfaces

Edward Miko

*V prispevku ugotovljamo, da parametri obdelave, kot so: podajanje na zob, vrtilna frekvenca, interval poti orodja in nastavni kot orodja, vplivajo na hrapavost površine pri frezanju s krogelnim frezalom. Za ugotavljanje in analizo morfologije tako obdelane površine smo uporabili vrstični elektronski mikroskop (VEM - SEM). V prispevku smo prikazali in obravnavali fotografije z VEM površine z vzdolžnim in prečnim profilom. Prav tako smo ocenili vpliv faktorjev obdelave na geometrijsko mikrostrukturo površine. Predstavili smo tudi frekvenčno analizo profila obdelane površine s krogelnim frezalom. Raziskave kažejo, da ima interval poti orodja znaten vpliv na hrapavost površine, obdelovane s frezanjem.*

© 2005 Strojniški vestnik. Vse pravice pridržane.

**(Ključne besede: frezanje oblikovno, obdelave površin, nastavljanje frezal, morfologija površin)**

*It has been established that machining parameters such as feed per tooth, rotational speed, tool path interval and cutter setting angle can influence the surface roughness during ball-end milling. A scanning electron microscope (SEM) was used to register and analyze the morphology of milled surfaces. SEM photographs of the surfaces with longitudinal and lateral profiles are included and discussed. The influence of the machining factors on the geometrical microstructure of the surface is also evaluated. A frequency analysis of the profiles of surfaces milled with a ball-end cutter is presented. The investigations show that the tool path interval has a considerable effect on the roughness of the milled surfaces.*

© 2005 Journal of Mechanical Engineering. All rights reserved.

**(Keywords: ball-end mill, surface finish, cutters, setting, surface morphology)**

#### 0 INTRODUCTION

Machining is a basic manufacturing technique used in mechanical engineering, and it is predicted that in the future its importance will not change. The amount of machining might even increase, as is in the case of precision machining [1].

Because of strong national and international economic competition, manufacturers are forced to introduce automation and flexible manufacturing, which increase the efficiency and the quality of products. The state of the superficial layer is one of the most important features of a product's quality. For this reason it is essential to be aware of the quality of the surface and attempt to improve it.

The improving accuracy of metal cutting, especially by turning and milling, means that machined surfaces often do not require any further finishing, which indirectly affects the operating properties of a product. Recently, a number of

producers have replaced the polishing of certain elements with an initial casting or forging process followed by turning or milling to obtain the final dimensions and surface finish by means of tools with ceramic and CBN wedges [2]. The constitution of the geometrical structure and the properties of the superficial layer generated by chip milling are important problems and, therefore, require further theoretical and experimental investigations. An important feature of the superficial layer quality is its roughness ([3] and [4]).

High-speed tracer milling (HSM) and contour milling performed by means of numerically controlled (CNC) milling machines are commonly used in the manufacturing of elements with complex shapes, such as casting and injection moulds, matrixes, blanking and press-forming dies, turbine blades, screw propellers and others ([5] and [6]). One of the most popular methods of milling is machining with a ball-end cutter, which enables, for example, full form

contouring on a CNC or tracer machine. No replacement of the tool is necessary, so the set-up and the machining time are much shorter. In the case of a 3-axis milling machine, it is desirable to use ball-end cutters that permit a quite different tool orientation in relation to the workpiece and, accordingly, machining a surface with complex 3D shapes [7]. Moreover, it would be essential to plan an optimum tool path for cutting, especially during the 3-axis milling of a 3D curvilinear surface. Milling with a ball-end cutter makes it possible to obtain a high, geometrical surface quality. Also, this type of milling can be applied to tasks once performed by EDMs (the milling of hardened materials or indenting). Therefore, machining with ball-end cutters has become interesting to many researchers and production engineers ([8] to [11]). A ball-end cutter is indispensable when it comes to the machining of surfaces inclined at a large angle [12].

Today, it is increasingly important that the form and the dimensional accuracy should be higher and the surface roughness should be lower. Therefore, face milling is being more and more frequently applied as a final treatment ([1] and [4]). Milling with a ball-end cutter can be used in the finishing of machine parts, if the requirements relating to surface quality are lower. However, the geometrical structure and the size of irregularities when a machined surface is subjected to further treatment are also of significance. The above factors will affect the machining time and related costs. In order to reduce the high labor consumption of finishing (usually manual polishing) [5], it is advisable to reduce as much as possible the surface irregularities after milling.

For these reasons, investigations have often focused on the evaluation of the influence of machining factors on the roughness of surfaces

machined with a ball-end cutter. Due to the fact that the surface's geometrical structure obtained after machining was non-homogeneous, the surfaces had to be evaluated using a scanning electron microscope. Measurements of the longitudinal and lateral roughness were also useful. In addition, the frequency of the longitudinal and lateral profiles of the milled surfaces were analyzed.

### 1 THEORETICAL SURFACE ROUGHNESS AFTER MILLING WITH A BALL-END CUTTER

The cutting edges of the cutter rotating around its own axis determine the axial-symmetrical area of the cutter's interaction. The machined surface is an envelope of the feed motion in the cutter interaction area. In the case of a ball-end cutter, the interaction area can have different shapes depending on the setting of the cutting part in relation to the workpiece. The cutter interaction area is also affected by the value of the depth of cut,  $a_p$ .

During ball-end milling, the tool touches the stock. The characteristic repeatable structure of the machined surface results from the path interval,  $a_c$  (i.e., the distances between particular paths). The structure reflects the height of surface irregularities (Fig. 1).

The height of the roughness,  $Rt$ , resulting from the path interval is the maximum roughness measured in the direction lateral to the milling direction and depends on the cutter diameter, the corner radius and the tool's cutting-edge angle (Fig. 1).

For a given path interval and tool diameter, the theoretical roughness height can be determined from the dependence:

$$Rt = \frac{D_c}{2} - \sqrt{\frac{D_c^2 - f_w^2}{4}} \quad (1),$$

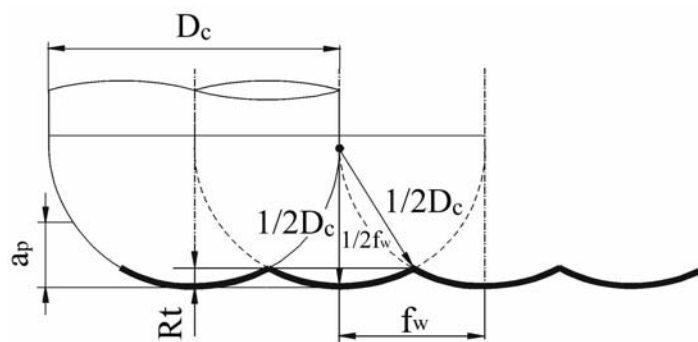


Fig. 1. Auxiliary diagram for determining the surface roughness parameters

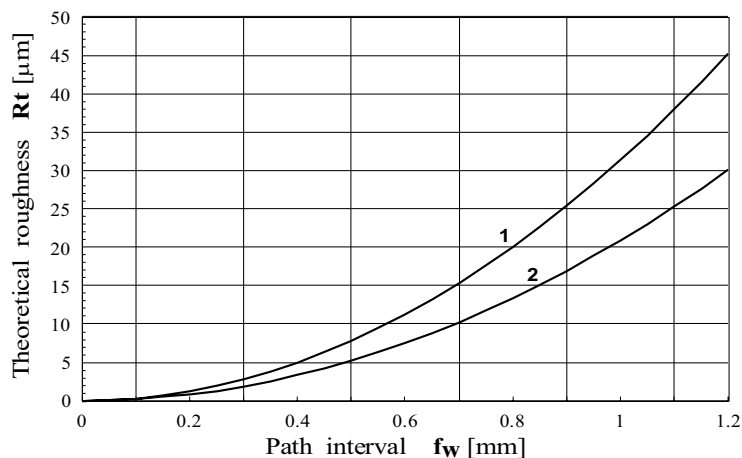


Fig. 2. Theoretical height of the surface roughness,  $R_t$ , in relation to the tool path interval,  $f_w$ , for a tool diameter of: 1,  $D_c = 8$  mm, and 2,  $D_c = 12$  mm

where  $D_c$  is the tool diameter, and  $f_w$  is the path interval.

The dependence of the height of the roughness,  $R_t$ , on the path interval,  $f_w$ , for diameters of ball-end cutter equal to  $D_c = 8$  mm and  $D_c = 12$  mm is presented in Fig. 2

The value of the mean arithmetic profile deviation from the mean line  $R_a$  can be defined from the relationship:

$$R_a = \frac{f_w^2}{9\sqrt{3} \cdot D_c} \quad (2).$$

The interdependence of the roughness,  $R_a$ , and the tool path interval,  $f_w$ , for cutters with diameters of  $D_c = 8$  mm and  $D_c = 12$  mm is presented in Fig. 3.

During ball-end milling, the cutting speed changes depending on the depth of cut,  $a_p$ . The depth of cut is connected with the term of the effective diameter,  $D_{ef}$ . The value of this diameter affects the cutting speed,  $v_c$ . For a given depth of cut it is the maximum cutting speed. If the depth of cut,  $a_p$ , is smaller than the radius  $R = D_c/2$  of the ball-ended tip, then the real diameter of the cutting tool,  $D_{ef}$ , can be calculated from:

$$D_{ef} = 2\sqrt{a_p(D_c - a_p)} \quad (3).$$

Figure 4 shows the dependencies of the effective diameter,  $D_{ef}$ , on the depth of cut,  $a_p$ , for a ball-end cutter with diameters of  $D_{c1} = 12$  mm and  $D_{c2} = 8$  mm.

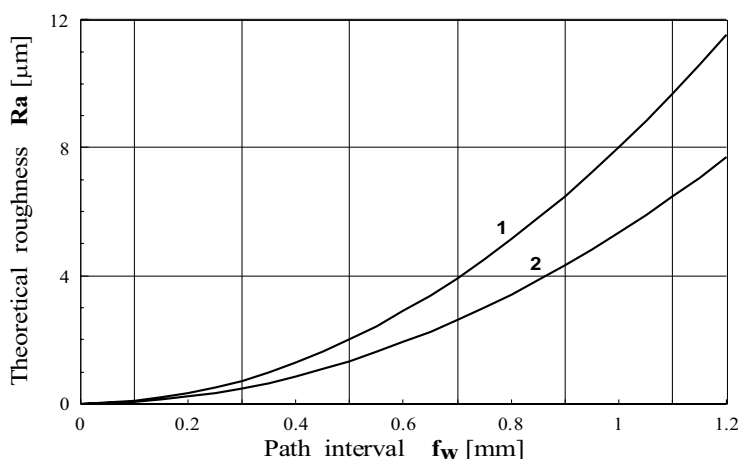


Fig. 3. Mean arithmetic profile deviation,  $R_a$ , in relation to the tool path interval,  $f_w$ , for a tool diameter of: 1,  $D_c = 8$  mm, and 2,  $D_c = 12$  mm

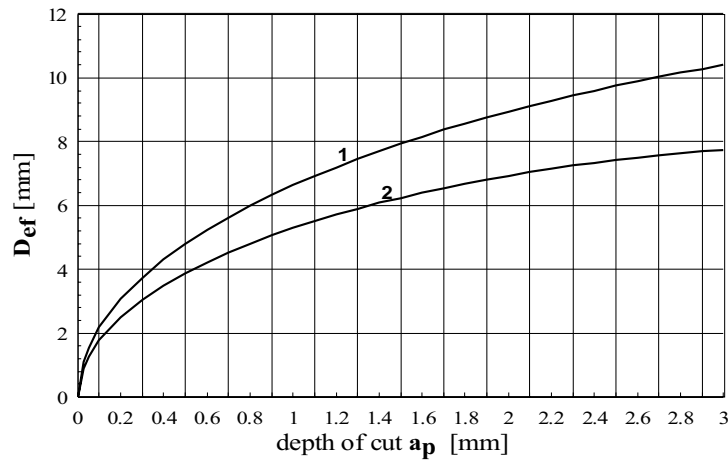


Fig. 4. Effective diameter of the cutting in relation to the depth of cut with a ball-end cutter with a diameter of: 1,  $D_{c1} = 12$  mm, and 2,  $D_{c2} = 8$  mm

Table 1. Cutting conditions for the studied samples

Cutting conditions	Tool - Heliball ball-end cutter made by ISCAR	
	CM D12 CR D120-QF-(IC328) insert	
Sample setting angle	0°	60°
Feed per tooth $f_z$ [mm/tooth]	0.04; 0.08; 0.12; 0.16; 0.20; 0.24	0.02; 0.04; 0.08; 0.12; 0.16; 0.20
Types of milling	In-cut, out-cut	In-cut, out-cut
Workpiece material	45 carbon steel, MO58 brass	
Tool rotational speed $n$ [rpm]	500; 1000; 1750; 2500; 3750; 4000	
Tool path interval $f_w$ [mm]	0.1; 0.3; 0.5; 0.7; 0.9; 1.1	

## 2 THE RESEARCH SUBJECT, RANGE AND METHODOLOGY

The aim of the research is to analyze the influence of selected machining factors on the roughness of surfaces milled with ball-end cutters on a CNC milling machine.

The samples were machined by applying the parameters given in Table 1. The machining was performed by changing one of the milling conditions, i.e., feed,  $f_z$ , tool path interval,  $f_w$ , or the rotational speed,  $n$ , and, accordingly, the cutting speed,  $v_c$ , and by milling with an appropriate part of the curvilinear edge of the insert.

The samples used in the experiments were made of 45 carbon steel (in accordance with the Polish standard No. - 93/H - 84019) and MO58 brass (in accordance with the Polish Standard No. 77/H - 87025). Their construction allowed a measurement of the longitudinal and lateral roughness.

Figure 5 shows the milling process and the method of sample fitting.

As soon as the cutting tests were completed and the specimens removed from the machine tool, longitudinal and lateral profiles of the roughness of the machined surface were registered and analyzed. In-cut and out-cut milling was performed on a CNC TRIAC 200 milling machine using Castrol syntilo RHS coolant. The applied CNC TRIAC 200 milling machine made by DENFORD was equipped with a 3-axis HEIDENHAIN 360 controller. The machining programs were generated with the MASTERCAM MILL system. Since the machine tool head cannot be turned, the samples were fitted in a specially designed machining holder. This enabled surfacing at 0° and 60° angles, which corresponded to the application of two different parts of the curvilinear edge of the cutter. A Heliball CMD120 ball-end cutter with a CRD12-QF-(IC328) double-edged insert 12 mm in diameter made by ISCAR was used for the machining.

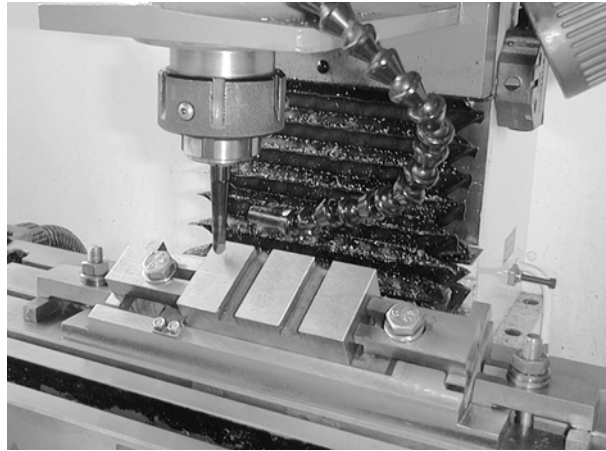


Fig. 5. View of milling of a specimen mounted in a machining holder at an angle of  $60^\circ$  using a CNC TRIAC 200 milling machine

The complex analysis of the geometrical surface structure ([4] and [10]) involved registration and study of the morphology of samples by means of a JEM-540 scanning electron microscope made by the Japanese company JEOL.

The research, divided into four stages, was conducted at the laboratories of the University of Technology in Kielce and the Institute of Metal Cutting in Cracow.

- The first part of investigations concerning machining was carried out at the Laboratory of Numerically Controlled Machine Tools, where by means of the MASTERCAM program the geometries of the specimens were prepared and CNC machining programs were developed. The programs were transmitted to a CNC TRIAC 200 milling machine, on which most tests, i.e., machining, were performed (Fig. 5). Two materials, 45 steel and MO58 brass, were used for machining and other tests.
- The next step was to measure the roughness,  $R_a$ , using a PM-03 profilometer in a room that satisfied the requirements given in the specifications of the device. The values of the lateral (perpendicular to the feed direction) and longitudinal (parallel to the feed direction) roughness were measured.
- At the third stage, the obtained surfaces were observed, evaluated and analyzed with respect to the microstereometry achieved by means of an scanning electron microscope. The observed surfaces of the brass and steel specimens were registered in a graphical file format that was attached to the investigation results.

- Finally, a PM-03 profilographometer was used to register and measure the lateral and longitudinal profiles. The POM-16 software was applied to determine the standardized unilateral functions of the spectral power density (FSPD) of these profiles.

The laboratory investigations were carried out at special stands, which enabled machining and measurement of the specimens and registration of the measuring results.

The test stand for machining the specimens consists of:

- a computer with the MASTERCAM MILL software,
- a CNC TRIAC 200 milling machine (Fig. 5),
- a workpiece.

The test stand for measuring the surface roughness includes:

- a tested-machined workpiece,
- a PM-03 profilometer for contact measurement of the roughness  $R_a$ .

The test stand for observing the surface morphology consists of:

- a JEM 5400 scanning electron microscope made by the Japanese company JEOL,
- a computer set and software for registering photographs.

The test stand for registering profiles and determining the FSPD consists of:

- a tested-machined workpiece,
- a PM-03 profilometer for contact measurement of the roughness  $R_a$ ,
- a computer set and the POM-16 software.

3 ANALYSIS OF THE RESULTS

Figures 6–9 show the influence of the studied factors on the lateral and longitudinal roughness,  $Ra$ , of 45 carbon-steel samples after machining with a ball-end cutter with a diameter of  $D_c = 12$  mm.

An increase in the tool path interval,  $f_w$ , causes an increase in the lateral roughness,  $Ra$  (Fig. 6). This figure shows the theoretical values of the parameter  $Rao$  determined from Eq. (2). One can see that the values measured on the surfaces machined at  $0^\circ$  and  $60^\circ$  angles are greater than the theoretical

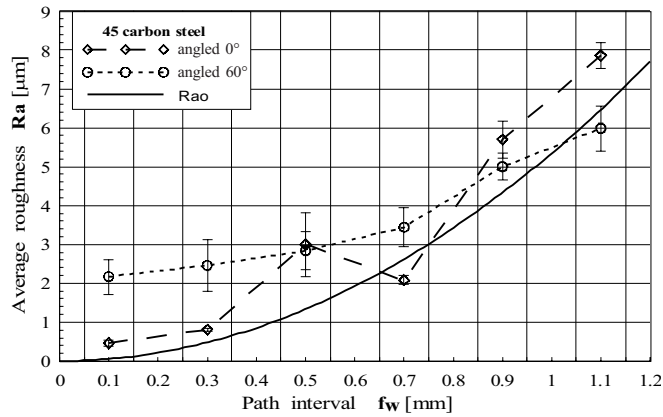


Fig. 6. Influence of the tool path interval,  $f_w$ , on the lateral surface roughness,  $Ra$ . The cutting conditions used were:  $a_p = 0.25$  mm,  $n = 2500$  rpm,  $f_z = 0.08$  mm/tooth,  $D_c = 12$  mm, in-cut milling

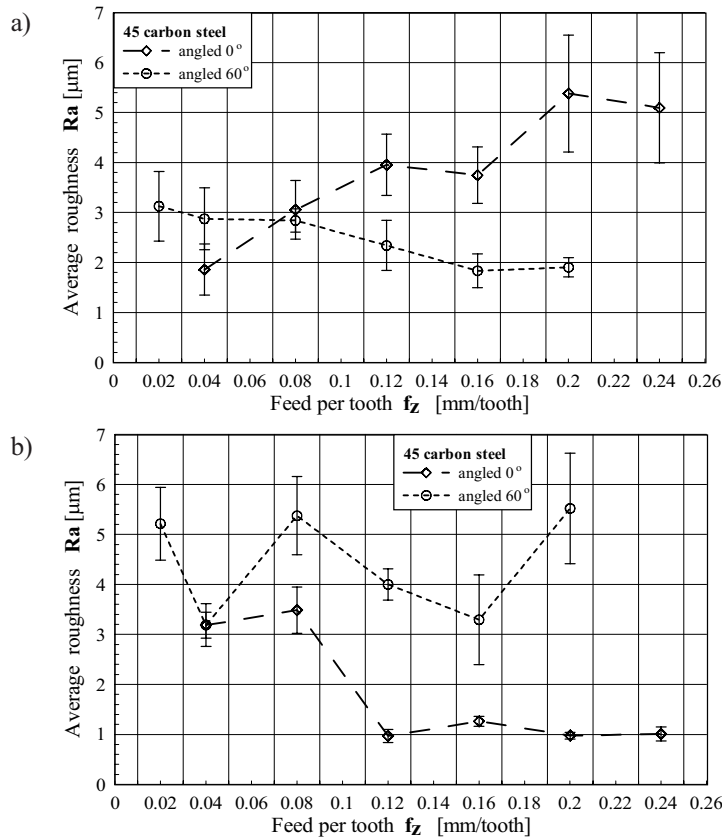


Fig. 7. Influence of the feed,  $f_z$ , on the lateral surface roughness,  $Ra$ . The cutting conditions used were:  $f_w = 0.5$  mm,  $a_p = 0.25$  mm,  $n = 2500$  rpm,  $D_c = 12$  mm; a) in-cut milling b) out-cut milling

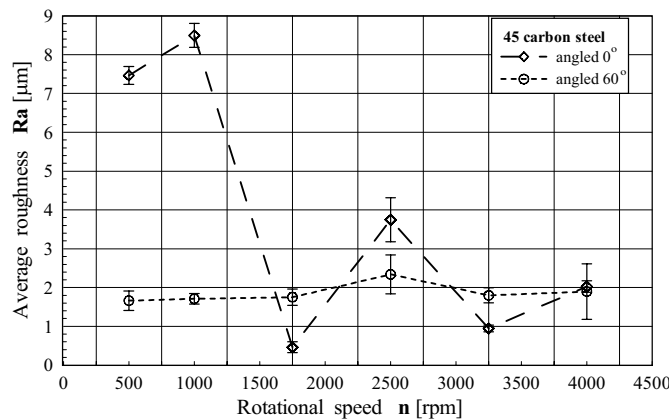


Fig. 8. Influence of the rotational speed,  $n$ , on the lateral surface roughness,  $Ra$ . The cutting conditions used were:  $f_w = 0.5$  mm,  $a_p = 0.25$  mm,  $f_z = 0.08$  mm/tooth,  $D_c = 12$  mm, in-cut milling

ones. Particularly large discrepancies occur for small tool path intervals,  $f_w$ . This confirms that other factors, foremost from the cutter-wedge representation, have considerable influence on the roughness of a machined surface. The factors include relative vibrations of the tool and the workpiece, the run-out of the cutter wedge and the plastic strain of the material.

During the in-cut milling of 45 steel, an increase in  $f_z$  causes an increase in the lateral roughness,  $Ra$ , when the sample is set at an  $0^\circ$  angle and its decrease at  $60^\circ$  (Fig. 7a). During out-cut milling, an increase in  $f_z$  results in a decrease in the value of the parameter  $Ra$  at  $0^\circ$  angle; yet no clear influence of  $f_z$  is observed at the  $60^\circ$  angle (Fig. 7b).

The cutter rotational speed,  $n$ , has no particular effect on the value of the parameter  $Ra$  when the angle of the setting is  $60^\circ$ . However, the influence is not clear at the downward trend and  $0^\circ$  angle (Fig. 8).

The effect of the feed,  $f_z$ , on the longitudinal roughness,  $Ra$ , is not clear during in-cut or out-cut milling (Fig. 9). In most cases, the roughness,  $Ra$ , was smaller after milling at a  $0^\circ$  angle than after milling at a  $60^\circ$  angle. A completely different situation was observed during milling with a single-wedge cutter with a diameter of  $D_c = 8$  mm [13]. During milling at  $0^\circ$  angle with a double-wedge cutter 12 mm in diameter for a given depth  $a_p = 0.25$  mm, only one wedge was used. At a  $60^\circ$  angle, however, two wedges were used. We can speculate that the increase in the roughness,  $Ra$ , was caused by the run-out of the cutter wedges. Despite the fact that at a  $0^\circ$  angle we have the effect of the small cutting speed and its unfavorable influence on the roughness, confirmed

during machining with a cutter 8 mm in diameter [13], the increase in roughness was smaller than when machining with a cutter 12 mm in diameter. The roughness was greater only when the 45 steel was milled at small values of rotational speed,  $n = 500$  and  $n = 1000$  rpm (Fig. 8), and great feeds at  $0^\circ$  angle rather than at  $60^\circ$  (Fig. 7b). This was probably due to a build-up edge, which is observed at the small cutting speed, and as such occurred for those revolutions and the  $0^\circ$  setting angle.

Figure 10 shows a photograph of surface morphology of a 45 carbon steel specimen machined with a ball-end cutter with a diameter of  $D_c = 12$  mm. The lateral and longitudinal profiles of the surface roughness can be seen on the left-hand side and at the top, respectively.

The presented out-cut milled surface has clear marks resulting from tool paths.

In a lateral profilogram the predominant frequency results from the tool path interval,  $f_w$ . The value of the roughness for this profile is  $Ra = 3.19 \pm 0.26$   $\mu\text{m}$  (Fig. 7b). The tool paths and the tool marks are also seen, and the intervals between them are equal to  $f_z$ . In a longitudinal profilogram the predominant frequency corresponds to the feed per tooth,  $f_z$ . The value of the parameter  $Ra$  for this profile is  $Ra = 2.42 \pm 0.30$   $\mu\text{m}$  (Fig. 9b). The frequency analysis of these profiles is shown in Figs. 12 and 13. Figure 11a is a photograph of a surface with tool marks magnified 90 times. Also, in Fig. 11b, where a magnification of 300 was applied, there are tool marks and boundaries of the material flow. Cracks and tears of the workpiece material are also observed.

The registered longitudinal and lateral profiles of the micro-roughness of the surfaces milled

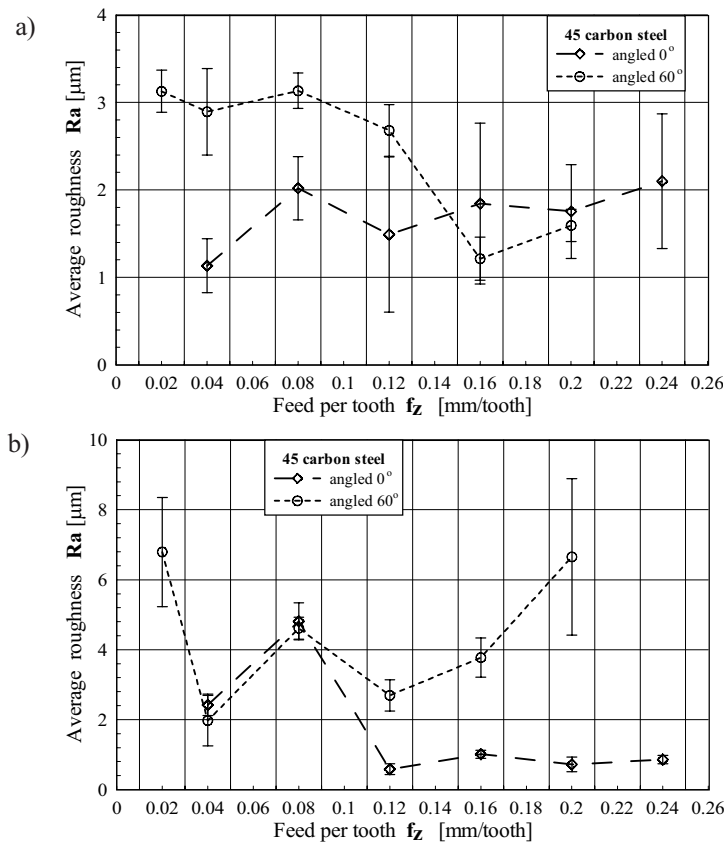


Fig. 9. Influence of the feed,  $f_z$ , on the longitudinal surface roughness,  $R_a$ . The cutting conditions used were:  $f_w = 0.5$  mm,  $a_p = 0.25$  mm,  $n = 2500$  rpm,  $D_c = 12$  mm; a) in-cut milling b) out-cut milling

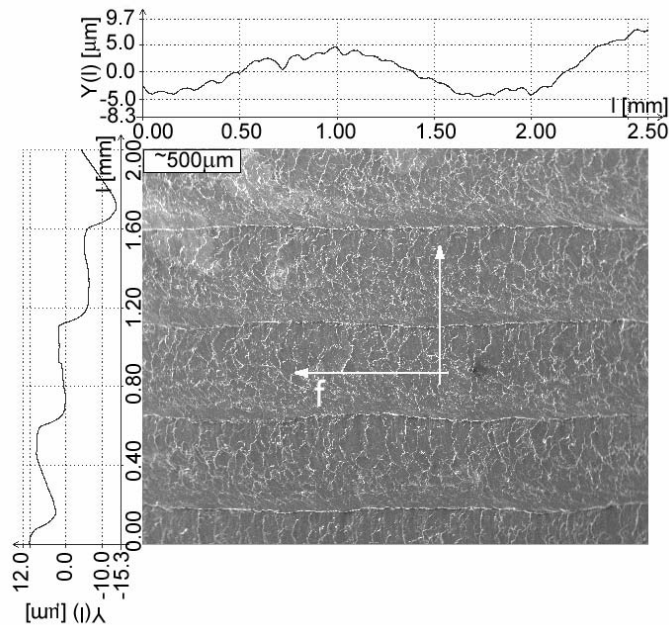


Fig. 10. Morphology and longitudinal and lateral profilograms of a surface machined with a ball-end cutter. The cutting conditions used were:  $f_z = 0.04$  mm/tooth,  $a_p = 0.25$  mm,  $f_w = 0.5$  mm,  $D_c = 12$  mm,  $n = 2500$  rpm, 45 steel workpiece material,  $0^\circ$  angle, out-cut milling. Magnification of 50



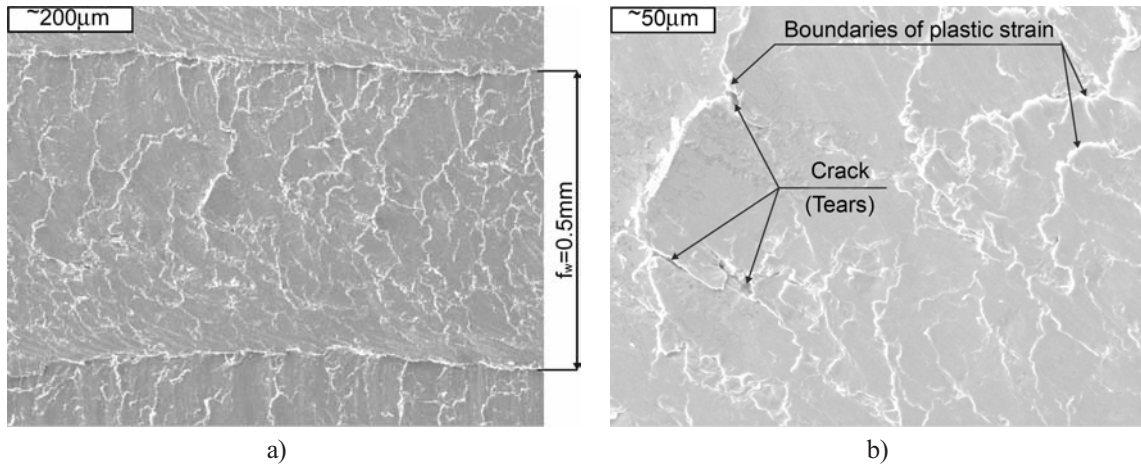


Fig. 11. Surface morphology. The cutting conditions used were:  $f_z = 0.2$  mm/ tooth,  $a_p = 0.25$  mm,  $f_w = 0.5$  mm,  $D_c = 12$  mm,  $n = 2500$  rpm, 45 steel workpiece material,  $0^\circ$  angle, out-cut milling; a) magnification of 90; b) magnification of 300.

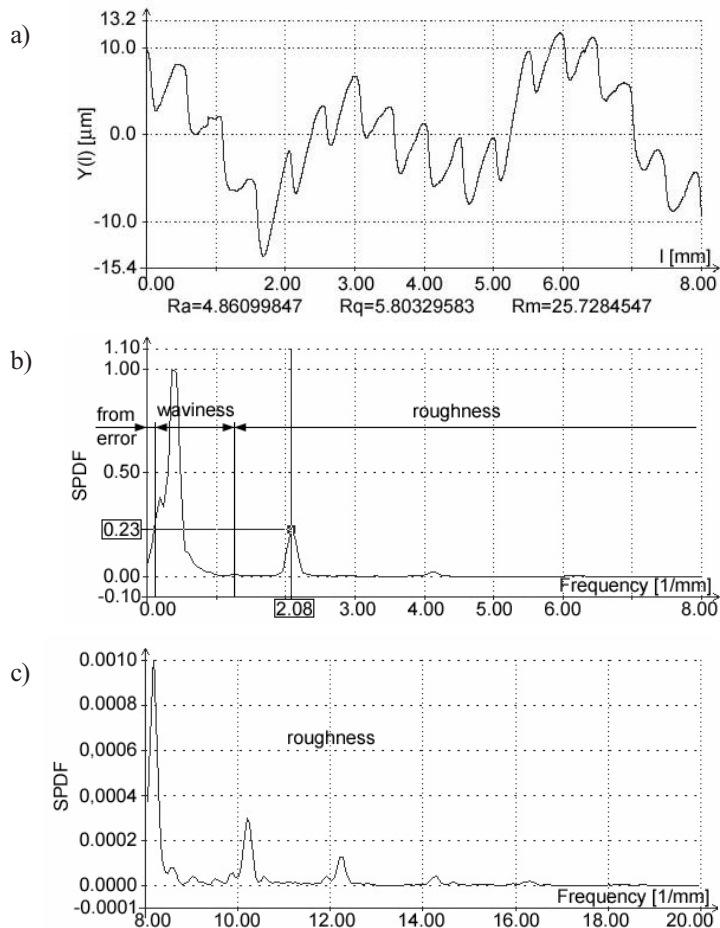


Fig. 12. Lateral profilogram (a) and the corresponding diagram of a standardized unilateral function of spectral power density of a profile (b, c). The cutting conditions used were:  $f_z = 0.04$  mm/tooth,  $a_p = 0.25$  mm,  $f_w = 0.5$  mm,  $D_c = 12$  mm,  $n = 2500$  rpm, 45 steel workpiece material,  $0^\circ$  angle, out-cut milling

according to the sampling plan (Table 1) were analyzed by determining a standardized unilateral function of the spectral power density (FSPD). The investigation results are presented in the form of profilograms and the corresponding FSPDs (periodograms), which define the profile frequency structure. In addition, in the FSPD diagrams, the ranges corresponding to the form and surface waviness and roughness errors are marked.

Bands corresponding to the tool path interval,  $f_w$ , were identified in the analyzed lateral periodograms, whereas the bands corresponding to the feed per tooth,  $f_z$ , were identified in the longitudinal ones.

Selected investigation results are presented in Figs. 12 and 13. Figure 12 shows a band with a frequency of 2.08 1/mm corresponding to  $f_w = 0.5$

mm, which is within the range of roughness. This means that, for the cutting conditions given in Fig. 12, this value of  $f_w$  will cause irregularities that are roughness. In Figs. 12 b and c subsequent harmonics of this band are seen. The influence of the tool path interval is predominant here.

Figure 13 presents a longitudinal profilogram and its frequency analysis. In Fig. 13b a band with a frequency of 0.8 1/mm situated within the range of waviness can be seen. The surface roughness, as the band indicates, is probably a result of errors of the machine tool table shift caused by the waviness of the shears of a Triac 200 milling machine. In Fig. 13c a band with a frequency of 24.29 1/mm was identified, which corresponds to a feed per tooth of  $f_z = 0.04$  mm/tooth. This figure shows a random character of the spectrum.

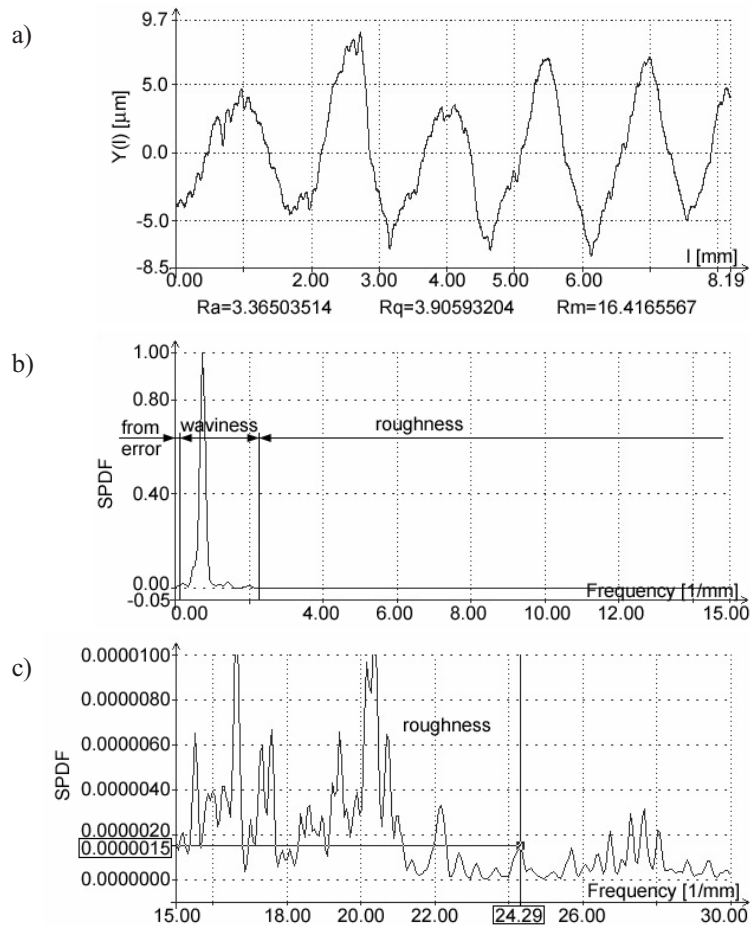


Fig. 13. Longitudinal profilogram (a) and the corresponding diagram of a standardized unilateral function of spectral power density of a profile (b, c). The cutting conditions used were:  $f_z = 0.04$  mm/ tooth,  $a_p = 0.25$  mm,  $f_w = 0.5$  mm,  $D_c = 12$  mm,  $n = 2500$  rpm, 45 steel workpiece material,  $0^\circ$  angle, out-cut milling

## 4 CONCLUSIONS

The comparative studies of the in-cut and out-cut ball-end milling using a cutter with a diameter of  $D_c = 12$  mm revealed that surface irregularities were smaller after in-cut milling.

Actually, when the diameter of the cutter is  $D_c = 12$  mm, smaller irregularities  $Ra$  are observed at a  $0^\circ$  angle (milling with the cutter tip) than at a  $60^\circ$  angle (milling with the cutter sides). We can speculate that the increase in roughness during milling with the cutter sides is probably caused by the run-out of the cutter wedges, which does not occur during milling with the cutter tip because, for such a setting and depth of cut  $a_p = 0.5$  mm, only one wedge is used. During milling with the cutter tip the effect of the low cutting speed is observed. It has an unfavorable influence on the surface roughness. In most cases, the effect of the run-out of the cutter wedges predominated over the effect of the low cutting speed, hence the irregularities of the surfaces milled with the cutter sides were usually greater than those milled with the cutter tip.

In the diagrams of the function of the spectral power density of the lateral profiles there are bands with a frequency corresponding to the value of the tool path interval and their subsequent harmonics. In the diagrams of the function of the spectral power density of longitudinal profiles there are bands with a frequency corresponding to the value of feed per tooth. In the diagrams we can also see a spectrum of a random character representing the influence of other factors of the machining system and the tool. The photographs of the machined surface present results of morphological investigations, i.e., the influence of a change of particular parameters ( $f_z, f_w, n$ ) on the character of the machined surface.

The photographs, where the feed was the key parameter, include, except for the evaluated surface, longitudinal and lateral profiles, testifying to difficult cutting conditions. In the photographs showing milling with the cutter tip ( $0^\circ$  angle) there are clear grooves, i.e., tool marks with unremoved material fragments and tears along the edges. This is caused by unfavorable cutting conditions near the tip, where the cutting speed is close to zero.

## 5 REFERENCES

- [1] Grzesik W. (1998) Podstawy skrawania materiałów metalowych. *WNT Warszawa*.
- [2] Jang D. Y., Choi Y. G., Kim H. G., Hsiao, A. (1996) Study of the correlation between surface roughness and cutting vibrations to develop an on-line roughness measuring technique in hard turning. *International Journal of Machine Tools and Manufacture*, vol. 36, Nr 4, 1996, s. 453 – 464.
- [3] Aronson R. B. (2001) Surface finish is the key to quality, *Manufacturing Engineering*, August 2001.
- [4] Nowicki B. (1991) Struktura geometryczna chropowatość i falistość powierzchni. *WNT Warszawa*.
- [5] Nowicki B. (1995) Automatyzacja obróbki wykańczającej powierzchni krzywoliniowych. *Mechanik*, nr 1, 1995, s. 5 - 9.
- [6] Altintas Y., Lee P. (1998) Mechanics and dynamics of ball end milling. *Transactions of ASME, Journal of Manufacturing Science and Engineering*, vol. 120, 1998, s. 684 – 692.
- [7] Altintas Y., Lee P. (1996) A general mechanics and dynamics model for helical end mills. *Annals of the CIRP*, vol. 45/1, 1996, s. 59 – 64.
- [8] Lim E. M., Menq CH. H. (1995) The prediction of dimensional error for sculptured surface productions using the ball- end milling process. Part 2: Surface generation model and experimental verification. *International Journal of Machine Tools & Manufacture*, vol. 35, nr 8, 1995, s. 1171 - 1185.
- [9] Lin R., Koren Y. (1996) Efficient tool path planning for machining free - form surfaces. *Transactions of the ASME, Journal of Manufacturing Science and Engineering*, vol. 118, 1996, s. 20 - 28.
- [10] Naito K., Ogo K., Konaga T., Abe T., Kanda K., Matsuoka K. (1994) Development of ball end milling for fine, high-efficiency finishing. *International Journal of the Japan Society for Precision Engineering*, vol. 28, nr 2, 1994, s. 105 - 110.
- [11] Olejarczyk K. (1994) Frezowanie łopatek narzędziami z ostrzami cermetalowymi i z regularnego azotku boru. *Mat. konf. I Forum prac badawczych „Kształtowanie części maszyn przez usuwanie materiału”*, Koszalin 1994, s. 168 - 174.

- [12] Chu C. N., Kim S. Y., Lee J. M., Kim B. H. (1997) Feed – rate optimization of ball end milling considering local shape features. *Annals of the CIRP*, vol. 46/1, 1997.
- [13] Miko E. (2001) Investigation into the surface finish in milling using a ball nose end mill. *Advances in manufacturing science and technology*, 25(2001)3, s. 71 - 86.

Author's Address: Dr. Edward Miko  
Mechanical Eng. and Metrology  
Kielce University of Technology  
Aleja Tysiąclecia Państwa  
Polskiego 7  
25-314 Kielce  
Poland  
emiko@tu.kielce.pl

Prejeto: 24.2.2005  
Received:

Sprejeto: 25.5.2005  
Accepted:

Odrpto za diskusijo: 1 leto  
Open for discussion: 1 year